Journal of Solid State Chemistry 211 (2014) 136–145

Contents lists available at ScienceDirect

Journal of Solid State Chemistry

journal homepage: www.elsevier.com/locate/jssc

A convenient strategy to functionalize carbon nanotubes with ascorbic acid and its effect on the physical and thermomechanical properties of poly(amide–imide) composites

Shadpour Mallakpour [a,b,*], Amin Zadehnazari [a]

[a] Organic Polymer Chemistry Research Laboratory, Department of Chemistry, Isfahan University of Technology, Isfahan 84156-83111, I.R. Iran
[b] Nanotechnology and Advanced Materials Institute, Isfahan University of Technology, Isfahan 84156-83111, I.R. Iran

ARTICLE INFO

Article history:
Received 29 October 2013
Received in revised form
13 December 2013
Accepted 19 December 2013
Available online 3 January 2014

Keywords:
Carbon nanotubes
Ascorbic acid
Electron microscopy
Mechanical properties
Thermal stability

ABSTRACT

Multi-walled carbon nanotubes (MWCNTs) were functionalized by ascorbic acid by a fast strategy under microwave irradiation to improve interfacial interactions and dispersion of CNTs in a poly(amide–imide) (PAI) matrix. This technique provides a rapid and economically viable route to produce covalently functionalized CNTs. The as-prepared, new type of functionalized CNTs were analyzed by several techniques. The thermal stabilities and mechanical interfacial properties of CNT/PAI composites were investigated using several techniques. The dispersion state of CNTs in the PAI matrix was observed by field emission scanning electron microscopy (FE-SEM) and transmission electron microscopy (TEM). The mechanical interfacial property of the composites was significantly increased by the addition of ascorbic acid treated CNTs. The FE-SEM and TEM results showed that the separation and uniform dispersion of CNTs in the PAI matrix. The overview of these recent results is presented.

1. Introduction

Carbon nanotubes (CNTs) have attracted much attention among scientists in a variety of disciplines since their discovery in 1991 [1]. These materials have diverse arrangements at a nanometric level that lead to different properties depending on the specific kind of nanotubes. CNTs display different properties that suggest potential for use in various advanced technological applications, such as tips for Atomic Force Microscopy [2], cells for hydrogen storage [3], nanotransistors [4], electrodes for electrochemical applications [5], sensors of biological molecules [6], catalysts [7], etc. Recently, much attention has been paid to the fabrication of composites with the use of CNTs in polymer materials to harness the exceptional intrinsic properties of CNTs [8–10]. Mechanical properties of CNTs suggest that they may be used as reinforcing materials in high-toughness nanocomposites, where stiffness, strength and low weight are important considerations [11]. There are numerous possible applications; some examples are aerospace structural panels [12], sporting goods [13], ultralightweight thin-walled space structures for use in space, and high stiffness-to-weight space mirror substrates [14]. In particular, polymers with the incorporation of CNTs show great potential for electronic device applications, such as nonlinear optics include protection of optical sensors from high intensity laser beams [15]. Additional applications involving the optical and electronic properties are organic field emitting displays, photovoltaic cells, highly sensitive strain sensors, electromagnetic interference materials, etc. [16–19]. Generally, there are two issues addressed in many previous studies: dispersion of CNTs in polymer matrix and interaction between CNTs and polymer. For the first issue, due to the high surface-to-mass ratio of CNTs, molecular scale forces and interactions should be considered among CNTs. Van der Waals forces usually promote flocculation of CNTs, whilst electrostatic charges or steric effects lead to a stabilization of the dispersion through repulsive forces [20]. As a consequence, by considering the nature of percolating network formed by very fine filler, e.g., CNTs, the balance of the two factors of reverse effects outlined above should be taken into account. For the second issue, the fact, that the nanotubes in the composites are coated or encapsulated by a thin insulating polymer layer, was identified for CNTs [21]. This encapsulation acts as a barrier to the electrical charge transfer between nanotubes. Actually, as-produced CNTs are almost insoluble in all media due to strong van der Waals interactions between tubes. Many approaches were employed to introduce functional groups covalently or noncovalently onto the surface of CNTs to facilitate the processing of the material [22–24]. Among

* Corresponding author at: Organic Polymer Chemistry Research Laboratory, Department of Chemistry, Isfahan University of Technology, Isfahan 84156-83111, I.R. Iran. Tel.: +98 311 391 3267; fax: +98 311 391 2350.
E-mail addresses: mallak@cc.iut.ac.ir, mallakpour84@alumni.ufl.edu, mallak777@yahoo.com (S. Mallakpour).

0022-4596/$ - see front matter © 2014 Elsevier Inc. All rights reserved.
http://dx.doi.org/10.1016/j.jssc.2013.12.021

the various surface modification strategies, covalent functionalization presents a possible strategy for the preparation of tubes with multifunctional properties and improved dispersability in a solvent. In the field of the nanocomposites, chemical functionalization offers an important tool in order to improve the interface and achieve the amazing properties that CNTs can provide. Different strategies for the functionalization of CNTs have been proposed, based on non-covalent and covalent bonding with many low-dimensional structures to the surface of CNTs [25,26].

Ascorbic acid (vitamin C) is a familiar molecule because of its dietary significance [27]. It is essential for the formation of intercellular collagen and therefore is required for the maintenance of tooth structures, cartilage, bone matrix the walls of capillaries and wound healing [28]. Ascorbic acid influences the formation of hemoglobin, erythrocyte maturation and certain immunological and biochemical reactions in the body. Vitamin C deficiency is rare in adults but may occur in infants, alcoholics or the elderly [29]. Deficiency leads to the development of scurvy. It has also played important roles in photosynthesis and photoprotection, in defense against ozone and other oxidative stresses and speculations about its role in cell expansion and cell division will be emphasized [30].

The specific objective of the present investigation is to provide ascorbic acid-functionalized multi-walled CNTs (MWCNTs-AS) for the first time under microwave irradiation and present evidences for the attachment between MWCNTs and ascorbic acid molecule. Multiple strategies, such as functionalization of MWCNTs and the use of an ultrasonication solution blending technique were adopted to disperse the MWCNTs-AS into a nanostructured poly (amide–imide) (PAI) matrix. Due to the introduction of several organic functionalities as well as aminophenol and amino acid groups, It can be expected that the chain packing distances increase and the intermolecular interactions decrease, leading to better interaction of the PAI chains with MWCNTs-AS and better dispersion of MWCNTs-AS in the PAI matrix. The influence of various MWCNT-AS distributions on the thermal and mechanical characteristics of PAI is also studied.

2. Experimental

2.1. Materials

Carboxylated MWCNTs synthesized by chemical vapor deposition (CVD) (the outer-diameter 8–15 nm, the inner-diameter 3–5 nm, length ~50 μm, carboxyl content 2.56 wt% and purity >95 wt%), were obtained from Neutrino Co. (Iran). Other chemicals were achieved commercially from Fluka Chemical Co. (Switzerland), Aldrich Chemical Co. (Milwaukee, WI) and Merck Chemical Co. (Germany). 4-Aminophenol, 3,5-dinitrobenzoylchloride, trimellitic anhydride (TMA), S-valine amino acid, glacial acetic acid, propylene oxide, tetrabutylammonium bromide (TBAB), and triphenyl phosphite (TPP) were used as received without further purification. Propylene oxide was used as acid scavenger. Hydrazine monohydrate and 10% palladium on activated carbon were used as obtained. N,N′-dimethylformamide (DMF) (d=0.94 g cm^{-3} at 20 °C), and N,N′-dimethylacetamide (DMAc) (d=0.94 g cm^{-3} at 20 °C) as solvents were distilled over barium oxide under reduced pressure before use. All other reagents were used as received from commercial sources.

2.2. Apparatus and measurments

The equipment used for the functionalization of MWCNTs and synthesis of the polymer was a Samsung microwave oven (2450 MHz, 900 W) (Seoul, South Korea). Melting points of the monomers were measured on a melting-point equipment (Gallenhamp, Cambridge, United Kingdom) without correction. ^{1}H nuclear magnetic resonance (NMR) spectrum was recorded on a Bruker (Rheinstetten, Germany) Avance 500 instrument at room temperature in dimethylsulfoxide-d_6 (DMSO-d_6). Multiplicities of proton resonance were designated as singlet (s), doublet (d), and multiplet (m). Fourier transform infrared (FT-IR) spectra of the samples were recorded with a Jasco-680 (Tokyo, Japan) spectrometer [taken in potassium bromide (KBr)] at a resolution of 4 cm^{-1}. They were scanned at wavenumber range of 400–4000 cm^{-1}. Band intensities were assigned as weak (w), medium (m), strong (s), and broad (br). Vibration bands were reported as wavenumber (cm^{-1}). Elemental analysis was performed in an Elementar Analysensysteme GmbH (Hanau, Germany). Inherent viscosity was measured using a Cannon Fenske Routine Viscometer (Mainz, Germany) at the concentration of 0.5 g/dL in DMF at 25 °C. Optical specific rotation was measured at the concentration of 0.5 g/dL in DMF at 25 °C using a quartz cell (1.0 cm) with a Jasco Polarimeter (JASCO Co., Ltd., Tokyo, Japan). Thermal stability of MWCNTs, PAI and MWCNT-AS/PAI nanocomposites was evaluated by recording thermogravimetric analysis (TGA) traces (STA503 TGA, Bahr-Thermoanalyse GmbH, Hüllhorst, Germany) in nitrogen atmosphere (flow rate 60 cm^3/min). A heating rate of 10 °C/min and a sample size of 10 ± 2 mg were used in each experiment. The X-ray diffraction (XRD) was used to characterize the crystalline structure of the samples. XRD patterns were collected using a Bruker, D8AVANCE (Rheinstetten, Germany) diffractometer with a copper target at the wave length of λ Cu$K\alpha$=1.54 Å, a tube voltage of 40 kV, and tube current of 35 mA. The samples were scanned at a rate of 0.05°/min from 10° to 80° of 2θ. For XRD studies, rectangular pellets prepared by compression molding were used. The morphology of the MWCNTs and dispersion morphology of the MWCNTs-AS on the PAI matrix were observed using field emission scanning electron microscopy (FE-SEM). The images were taken at 15 kV using a HITACHI S-4160 instrument (Tokyo, Japan). Transmission electron microscopy (TEM) images were obtained using a Philips CM 120 microscope (Netherlands) with an accelerating voltage of 100 kV. For TEM studies, ultra-thin sections (30–80 nm) of MWCNTs-AS and the composites were prepared using Leica Ultramicrotome. Tensile testing was performed at room temperature on a Testometric Universal Testing Machine M350/500 (Mainz, Germany), according to ASTM D 882 (standards). Tests were carried out with a cross-head speed of 12.5 mm/min until reaching a deformation of 20% and then, at a speed of 50 mm/min at break. The dimensions of the test specimens were 35 × 2 × 0.04 mm^3. Property values reported here represented an average of the results for tests run on at least five specimens. Tensile strength, tensile modulus, and strain were obtained from these measurements. The composites were prepared by using a MISONIX ultrasonic XL-2000 SERIES (Raleigh, North Carolina, USA). Ultrasonic irradiation was performed with the probe of the ultrasonic horn being immersed directly in to the mixture solution system with the frequency of 2.25 × 10^4 Hz and the power of 100 W.

2.3. Monomer synthesis

N-trimellitylimido-S-valine (3) was prepared according to our previous work [31]. 3,5-Diamino-N-(4-hydroxyphenyl)benzamide (7) as a diamine monomer was also prepared according to our reported procedure (Scheme 1) [32].

2.4. Functionalization of MWCNT

The reaction sequence for the ascorbic acid-functionalized MWCNTs is shown in Scheme 2. Ascorbic acid (200 mg, 1.13 mmol) was dissolved in 15 mL of DMAc. After addition of 100 mg

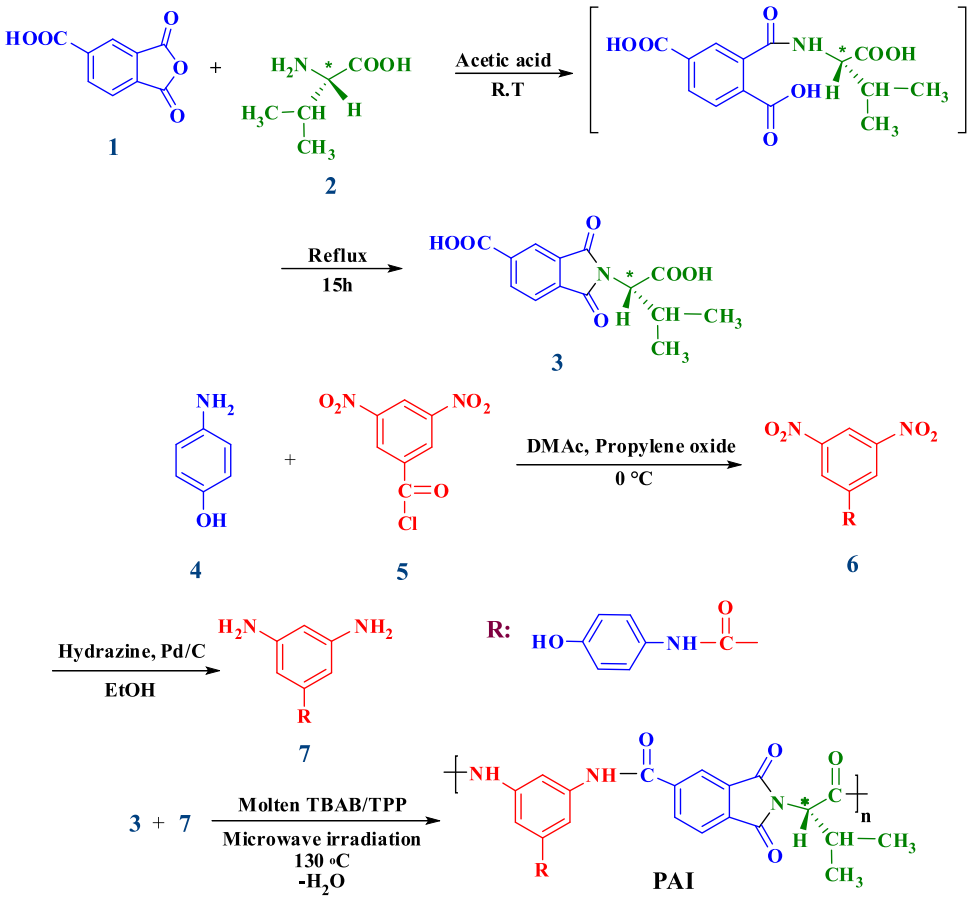

Scheme 1. Synthetic route used to obtain the PAI.

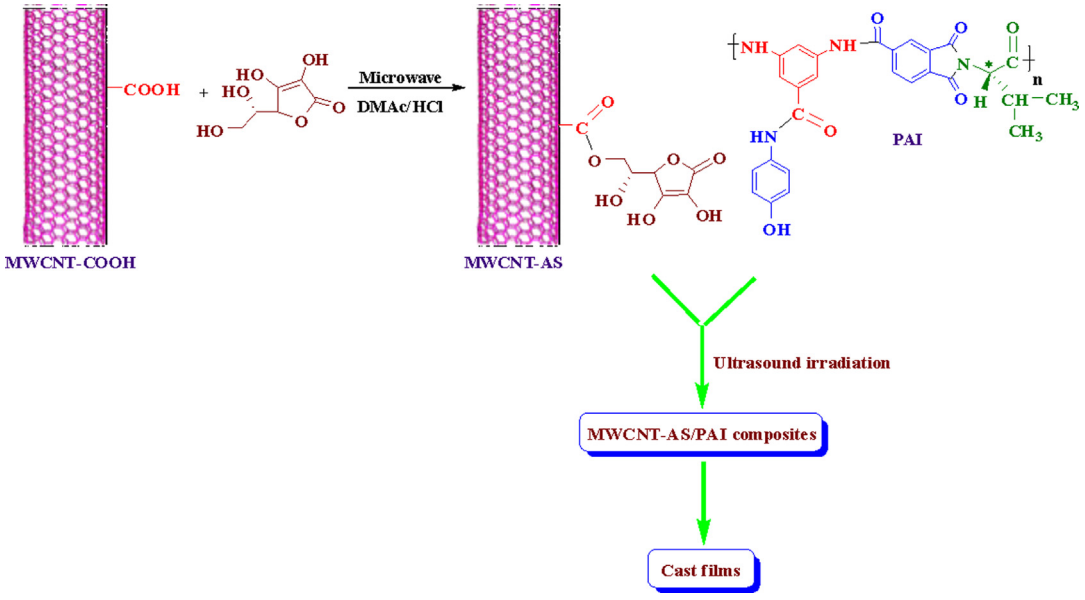

Scheme 2. Schematic representation of the attachment of vitamin C with MWCNTs and preparation of their PAI-based composites.

carboxylated-MWCNT and 0.10 mL of conc. HCl, the solution was reacted at 80 °C for 2 h. The suspension was then poured into a porcelain dish (50 mL) and placed in a domestic microwave chamber. The abovementioned MWCNTs suspension was heated in microwave up to 120 °C for 15 min with output power of 700 W. Then the resulting suspension was cooled to room temperature and poured into 200 mL of water. The mixture was stirred for 30 min at room temperature and then decanted to remove the solvent. When the amount of solvent became about 20 mL, the mixture was subjected to irradiation with high-intensity ultrasound for 1 h. The obtained homogeneous suspension was placed in an 80 °C oven overnight to evaporate most of the solvent.

The filtration products were washed more than 7 times with water for the removal of any unreacted residue of vitamin C, and dried under vacuum to give the product of MWCNT-AS.

2.5. Polymer synthesis

About 0.10 g (3.43×10^{-4} mol) of diacid monomer 3, 0.08 g (3.43×10^{-4} mol) of diamine 7, and 0.44 g of TBAB (1.37×10^{-3} mol) were placed in a porcelain dish and ground completely for 5 min; then, 0.36 mL (1.37×10^{-3} mol) of TPP was added and the mixture was ground for 3 min. The reaction mixture was irradiated in the microwave oven for 8 min at 50% of power level (900 W) (the temperature of the reaction was around 130 °C). The resulting viscous solution was poured into 30 mL of methanol, filtered, and dried at 80 °C for 6 h under vacuum to give 0.17 g (96%) of yellow powder PAI. The optical specific rotation was measured ($[\alpha]^{25}_{Na,589} = -42.18^{\circ}$) at a concentration of 0.5 g/dL in DMF at 25 °C. The inherent viscosity was also measured (η_{inh} = 0.32 dL/g) under the same conditions.

FT-IR (KBr, cm^{-1}): 3302 (m, br, NH and OH stretching), 3101 (w, C–H aromatic), 2964 (w, C–H aliphatic), 2927 (w, C–H aliphatic), 1777 (m, C=O imide, asymmetric stretching), 1719 (s, C=O imide, symmetric stretching), 1665 (s, C=O amide, stertching), 1601 (s), 1544 (s), 1512 (s), 1446 (s), 1377 (s, C–N–C axial stretching), 1210 (m, C–N–C transverse stretching), 1071 (m), 865 (m), 835 (s), 757 (m), 727 (s, C–N–C out-of-plane bending), 687 (w), 526 (w). ^{1}H NMR (400 MHz, DMSO-d_6, ppm): 0.89 (d, 3H, CH_3, distorted), 1.08 (d, 3H, CH_3, distorted), 2.84 (m, 1H, CH), 4.64–4.66 (d, 1H, CH, J=7.60 Hz), 6.73 (s, 1H, Ar–H), 7.19 (s, 1H, Ar–H), 7.28–7.30 (d, 2H, Ar–H, J=8.00), 7.47–7.49 (d, 2H, Ar–H, J=8.00 Hz), 7.75 (d, 1H, Ar–H, distorted), 7.99 (s, 1H, Ar–H), 8.09–8.11 (d, 1H, Ar–H, J=7.20 Hz), 8.45 (s, 1H, Ar–H), 9.26 (s, 1H, OH), 10.18 (s, 1H, NH), 10.80 (s, 2H, NH), 10.88 (s, 2H, NH).

Elemental analysis: calculated for $(C_{27}H_{22}N_4O_6)_n$: C, 65.05%; H, 4.45%; N, 11.24%. Found: C, 64.90%; H, 4.41%; N, 11.07%.

2.6. Preparation of the MWCNT-AS/PAI composite films

Initially, PAI was dissolved and MWCNTs-AS was separately dispersed in DMAc with stirring being for 1 day at 30–40 °C. Then, two stock solutions were mixed to achieve the desired weight percentages of MWCNTs-AS from 5 to 15 wt%. The MWCNT-AS/PAI mixture was stirred for 1 day at 30–40 °C and then ultrasonicated in a water bath for 1 h. To remove the DMAc solvent, MWCNT-AS/PAI mixture was poured into uncovered preheated glass Petri dishes and uniformly heated at 60 °C for 1 day; then the semidried film was further dried in vacuum at 160 °C for 8 h in order to remove the residue solvent and a solid film was formed. Composite films formed after the evaporation of DMAc could be easily lifted from the glass Petri dishes. Freestanding polymer films with 50 μm thickness were then peeled from the glass plate and subjected to different tests.

3. Results and discussion

3.1. Synthesis and structural characterization of monomers

Diacid monomer 3 was synthesized by the condensation reaction of an equimolar amount of TMA and S-valine in refluxing acetic acid solution (Scheme 1) [31]. Diamine monomer 7 was synthesized using a two-step process (Scheme 1) [32]. In the first step, aromatic nucleophilic displacement of 3,5-dinitrobenzoylchloride with 4-aminophenol in the presence of propylene oxide in DMAc solvent resulted in dinitro compound 6 as a yellow solid. In the second step, this dinitro was reduced in ethanol in the presence of hydrazine hydrate and a catalytic amount of palladium on the activated carbon at 80 °C to produce yellow crystals of the diamine 7. The structure of the dinitro 6 and diamine 7 was identified by elemental analysis, FT-IR, ^{1}H NMR, and ^{13}C NMR spectroscopy.

3.2. Polymer synthesis

A synthetic strategy, using molten TBAB and microwave irradiation collectively, was found to be a successful and efficient method for the synthesis of polymer. The monomers (3 and 7) mixtures were irradiated under microwave (optimized condition; 50% of power level, 130 °C) with TBAB in the presence of TPP for 8 min. The polymer precipitated in a powder form when slowly pouring the resulting polymer solution under stirring into methanol. It was observed that the PAI was obtained in 94% of isolated yield. Thus, we found that molten TBAB salt was a highly polar medium that was likely to be a strong microwave absorption. The inherent viscosity of the synthesized PAI was 0.48 dL/g. The resulting polymer showed optical rotation, which indicated that the polymer was optically active and chirality was introduced into the backbone of the polymer. The optical specific rotation of this polymer was $[\alpha]^{25}_{Na,589} = -35.1^{\circ}$ (0.05 g in 10 mL of DMF). Elemental analysis, FT-IR and ^{1}H NMR spectroscopy were used to confirm the formation of PAI [33].

3.3. Functionalization of MWCNTs

We have previously reported on the functionalization of MWCNT with several organic functionalities [34–38]. Accordingly, vitamin C was selected to react with MWCNTs. The reaction sequence is depicted in Scheme 2. Functionalization was carried out under microwave irradiation. The optimum microwave power level and period of heating were selected according to our previous work [34]. An esterification reaction occurred between the ascorbic acid molecule and carboxylic acid group of the MWCNT's surface under microwave irradiation. The separation and purification of products, is carried out easily and in a convenient way by simple decanting. The resulting paste was washed with DMAc and water, sonicated and dried.

3.4. Composite films preparation

The dispersion of the MWCNTs-AS in 5, 10, and 15 wt% solutions of PAI in DMAc was attained by a vigorous stirring with a speed of 15,000 rpm for 1 day, using a homogenizer, which was followed by utrasonication process for 1 h to form a new series of MWCNT/PAI composites. The reaction pathway for preparing MWCNT-AS/PAI composites is shown in Scheme 2. The effective use of CNTs in composite applications depends on the ability to disperse the CNTs homogeneously throughout the matrix without reducing their aspect ratio. Due to the van der Waals attraction, CNTs are held together as bundles and ropes. Therefore, they have a very low solubility in solvents and tend to remain as entangled agglomerates. To employ CNTs as an effective reinforcement in polymer composites and ensure proper dispersion and appropriate interfacial adhesion between the CNTs and polymer matrix, several mechanical/physical methods were used [39,40]. So, in this study, at first, the MWCNTs were functionalized with ascorbic acid. Several researches have recently investigated the properties of CNT/polymer composites with CNT content from 1 to 15 wt% and good results have been obtained and reported [41–43]. From this point of view, we selected 5%, 10%, and 15% of CNT content in the composites. The lower level of aggregation in the modified CNTs can be attributed not only to the presence of functional groups such as ascorbic acid groups but to their high aspect ratio.

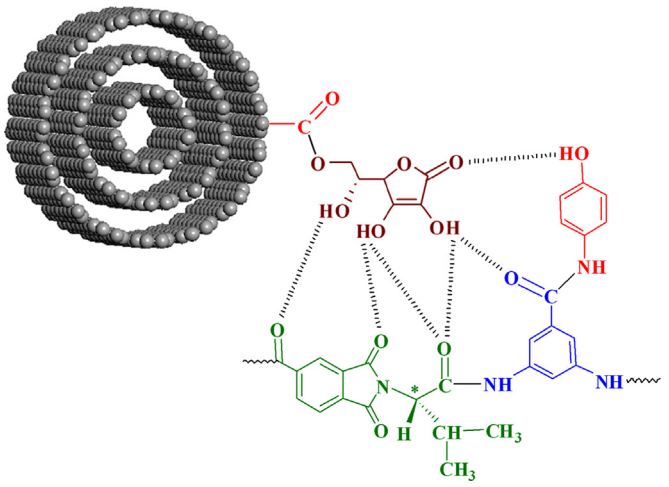

Fig. 1. Presentation of possible interactions of hydrogen bonding between the MWCNT-AS and the PAI chains.

This transformation should contribute positively to the good dispersion of CNTs in the PAI matrix. Moreover, the introduction of several functional groups into the backbone of aromatic polymer performs a hydrogen bonding with modified CNTs and a composite based on hydrogen bond by which PAI chains are tightly attached to the surface of MWCNT-AS. Possible interactions between PAI chains and MWCNT-AS are described in Fig. 1.

3.5. Characterization of MWCNTs and the composites

3.5.1. Structural data

The spectral analysis data indicated the successful incorporation of ascorbic acid onto MWCNT surfaces through esterification reaction. Fig. 2 shows FT-IR spectra of the MWCNT-COOH and the MWCNT-AS. The organic moieties of MWCNT-AS was characterized with the absorptions of the –OH groups at 3425 cm^{-1}, –CH groups at 2926 cm^{-1}, –COO– groups at 1735 cm^{-1}, and –C–O– groups at 1118 cm^{-1} in its FT-IR spectrum. The spectrum of a carboxylated MWCNTs/KBr pellet showed a strong, broad absorption band centered at 3433 cm^{-1}, which could be related to the stretching vibration of O–H bands of carboxylic acid moieties from the surface of MWCNTs. The small peak around 2923 cm^{-1} was ascribed to aliphatic sp^3 C–H of MWCNTs [44]. Strong band of absorption characteristic for the acid linkage appeared at 1629 cm^{-1} assigned to C═O stretching vibration. The structure of PAI was also confirmed by using FT-IR spectroscopy. Strong absorption bands were observed at 1777 cm^{-1}. This can be related to the asymmetric and symmetric stretching vibrations of the imide carbonyl groups. The bands of C–N bond stretching and ring deformation appeared at 1377 and 727 cm^{-1}. Strong bands of absorption were characteristic of the hydroxyl groups and the newly formed amide linkage appeared at around 3302 cm^{-1}. They were assigned to O–H and N–H stretching vibrations at 1665 cm^{-1}, which can be attributed to amide C═O stretching vibration, and at 1544 cm^{-1}, they were due to N–H bending vibration. The absorption band at around 3101 cm^{-1} was attributed to ═CH aromatic linkage. The aliphatic C–H stretching peak was also appeared at around 2964 cm^{-1} [45]. The presence of MWCNTs-AS in the polymer matrix showed very few changes in the FT-IR spectrum, presumably due to the low MWCNT-AS composition and the weak vibration signals of MWCNTs. Fig. 2 shows the representative FT-IR spectrum of MWCNT-AS/PAI 15 wt%.

The structure of neat PAI was also studied by ^1H NMR spectroscopy. The presence of the –NH protons of amide groups at 10.18, 10.80, and 10.88 ppm as three singlet peaks, and –OH group at

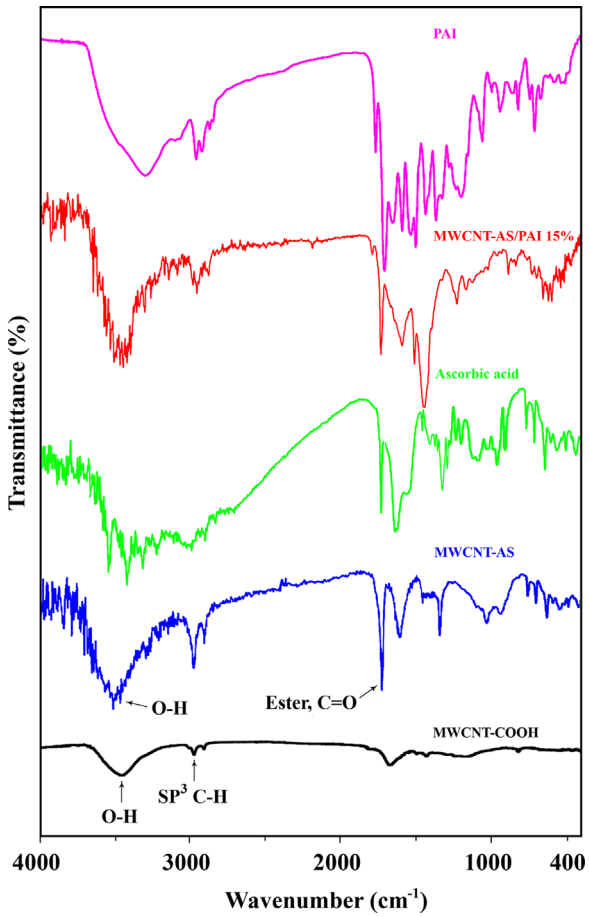

Fig. 2. FT-IR spectra of MWCNT-COOH, MWCNT-AS, PAI, and the composite containing 15 wt% of MWCNT-AS.

9.26 ppm as a singlet peak, respectively, indicated the presence of amide groups in the polymer's side chain as well as main chain and hydroxyl groups in the polymer's side chain. The resonance of aromatic protons appeared in the range of 6.73–8.45 ppm. The proton of the chiral center appeared as doublet at 4.64–4.66 ppm.

3.5.2. XRD

To further study the structure of the MWCNT/PAI nanocomposites, the XRD characterizations of MWCNTs, the pure PAI, and the MWCNT/PAI nanocomposites with 5, 10, and 15 wt% of MWCNTs content were conducted (see Fig. 3). In the case of MWCNTs, three peaks appeared at $2\theta = 26^\circ$ and 44°, which are typically associated with diffraction metal impurities ($2\theta = 26^\circ$ corresponds to the (0 0 2) diffraction plane of the impurity graphite, and $2\theta = 44^\circ$ to α-Fe (1 1 0) and/or Ni (1 1 1) diffractions [46]). MWCNTs-AS showed very few changes in the XRD pattern. It could be seen that XRD pattern is very similar to the carboxylated MWCNTs. MWCNTs-AS still had the same cylinder wall structure as raw MWCNTs and inter-planner spacing of all samples remained the same. As for the pure PAI, an obvious broad peak centered at 20° indicates that PAI is amorphous. The XRD patterns of the MWCNT/PAI composites appeared the both the characteristic peaks of the pure PAI and MWCNTs. Moreover, the intensity of the peaks assigned to the MWCNTs in the composite increased with the increase of the content of MWCNTs. However, the position of the peaks corresponding to the two constituents of the composite was same to the individual of PAI and MWCNTs, which illustrated that either the orientation of the PAI chains or the structure of

MWCNTs was not affected by each other along the process of fabrication.

3.5.3. FE-SEM

The typical microstructure of the unmodified and modified MWCNTs investigated by FE-SEM is presented in Fig. 4. The FE-SEM image of the MWCNTs-COOH surface is approximately smooth. After functionalization with ascorbic acid, the surface of MWCNTs became a rough and debundled structure, as can be seen in Fig. 4. FE-SEM images of neat PAI and composites were also examined to characterize the morphology and dispersity of MWCNTs-AS in the composites, as displayed in Fig. 5. The neat PAI copolymer showed spherical particles which were self-organized into a nanoscale size. The average diameter of polymeric particles was about 36 nm. For MWCNT-AS/PAI composites, MWCNTs-AS were well dispersed and embedded in the PAI matrix without showing noticeable MWCNT-AS aggregation.

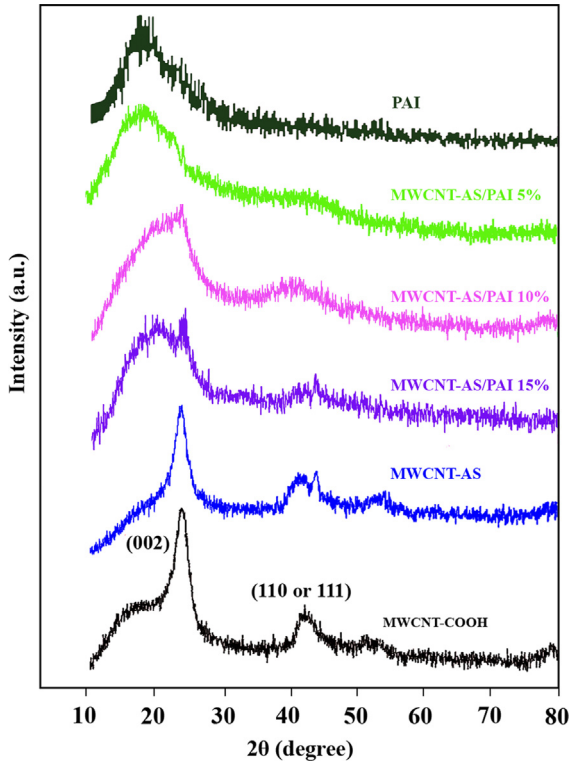

Fig. 3. XRD pattern for MWCNT-COOH, MWCNT-AS, and MWCNT-AS/PAI composites samples with different MWCNT-AS content.

3.5.4. TEM

The TEM images of the MWCNT-AS are presented in Fig. 6. The images show a high surface roughness which implies the partial damage of graphitic carbon. This phenomenon could have resulted from the severe functionalization or oxidation processes [47]. Although TEM could not distinguish minute functional groups, it could represent surface deterioration of the CNTs that occurred as a result of functionalization. As mentioned above, the functionalization reaction disrupted the sp^2 carbon network of graphitic CNTs, so it may be responsible for the roughness of CNTs' surfaces. In fact, since the microwave radiation was harsh enough to produce highly disordered carbon (Fig. 6), it is likely that it could also damage graphitic MWCNTs [48]. Fig. 7 is the TEM observation of the dispersion of the modified MWCNTs in the PAI matrix (mass fraction of MWCNTs is 10 wt.%). It can be seen that the MWCNTs were almost attached to the polymeric particles, resulting from the increased polarity by the functional groups formed on the surfaces of MWCNTs as well as carbonyl groups in the PAI structure. Possible interactions between the carboxyl groups at the MWCNT-AS with the oxygen atom at the carbonyl groups of the PAI are shown in Fig. 1.

3.5.5. TGA

Fig. 8 gives the TGA curves of the nanocomposites, pure PAI, and MWCNTs. The results obtained from these curves are completely tabulated in Tables 1 and 2. Single step degradation was observed in all samples. The curve of pristine CNT showed a small mass loss in a temperature range of 0–550 °C. The weight loss of

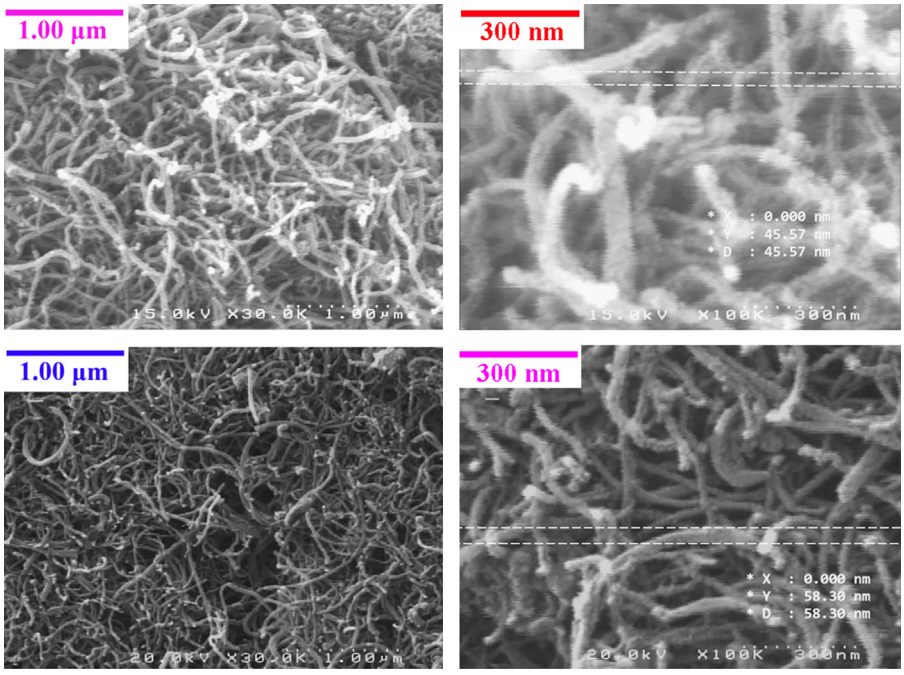

Fig. 4. FE-SEM micrograph of MWCNT-COOH (top) and MWCNT-AS (bottom).

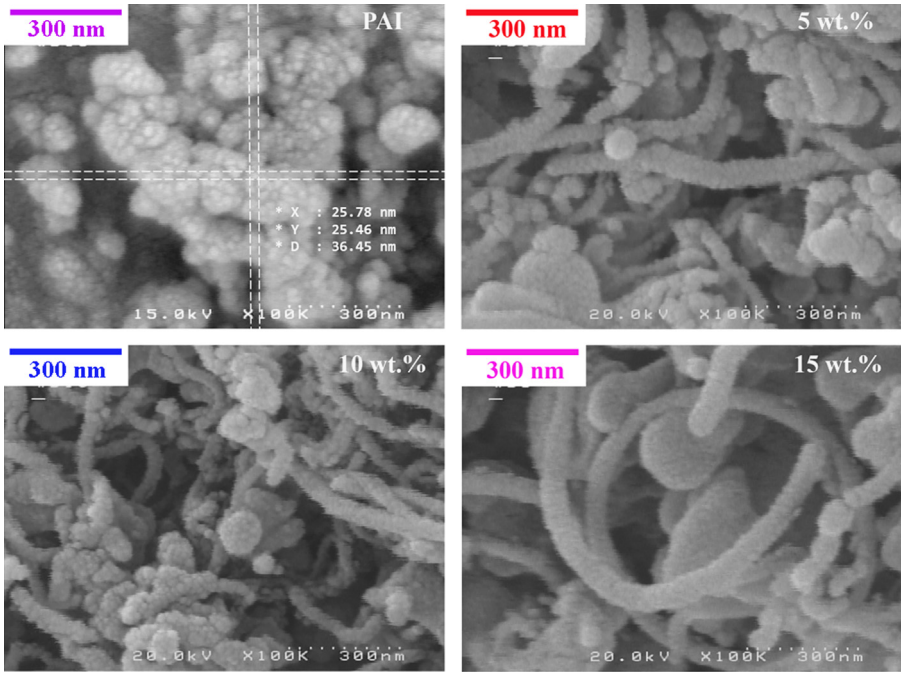

Fig. 5. FE-SEM micrographs of: (a) neat PAI and composites containing (b) 5 wt%, (c) 10 wt%, and (d) 15 wt% of MWCNTs-AS.

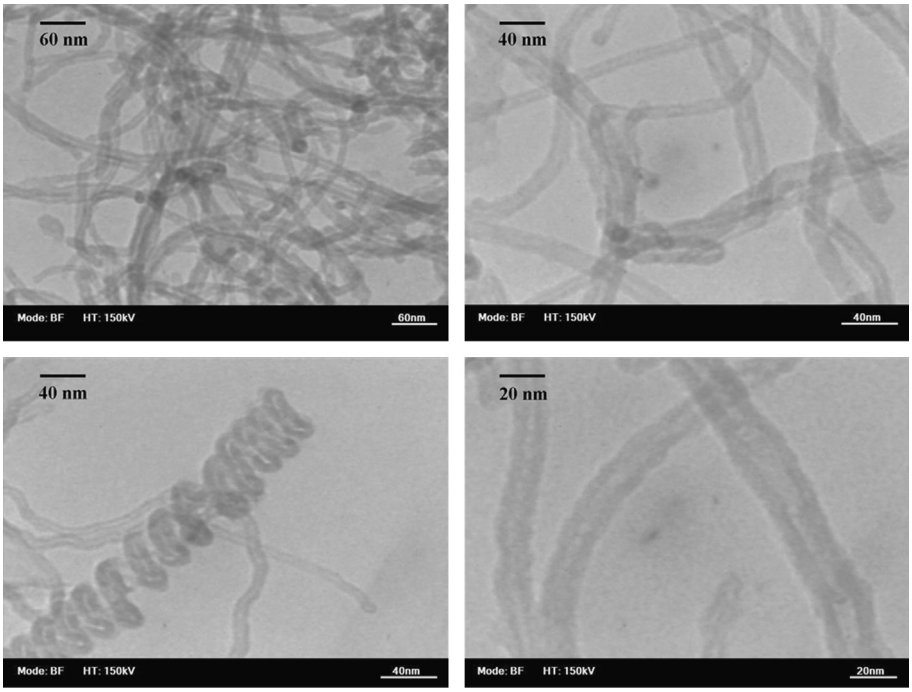

Fig. 6. TEM images of MWCNT-AS at different magnifications.

MWCNT-AS resulted from the decomposition of the functionalized organic moieties attached to the surface of MWCNTs. TGA data of the pristine and the purified MWCNTs suggested that the MWCNTs were able to withstand oxidation temperatures up to 700 °C. This could be due to the incorporation of carboxyl groups in the defective sites and tips. The initial decomposing temperature of the MWCNT-COOH was 550 °C, indicating that the MWCNTs-COOH were thermally stable up to this temperature, as shown in Table 1. The modified MWCNTs decomposed slowly from 220 °C because of the losing organic groups on the surface of MWCNTs. By comparing the MWCNTs-AS with MWCNTs-COOH, it can be concluded that the thermal stability of MWCNTs-COOH was destroyed upon functionalization with ascorbic acid. The thermal behavior data for the PAI and the composites are summarized in Table 2. The thermal stability of the MWCNT/PAI composites increased linearly with increasing MWCNT-AS content. This could be related to the higher thermal conductivity of CNTs that facilitated heat dissipation within the composites, hence preventing the accumulation of heat at certain points for degradation [49]. The end temperature of decomposition was also retarded with increasing MWCNT-AS content. The weight percent remaining after major degradation at 800 °C was higher for composites rather than neat PAI. This indicated that MWCNT reduced the degradation of PAI at high temperature as the effect was clearly seen in the curves.

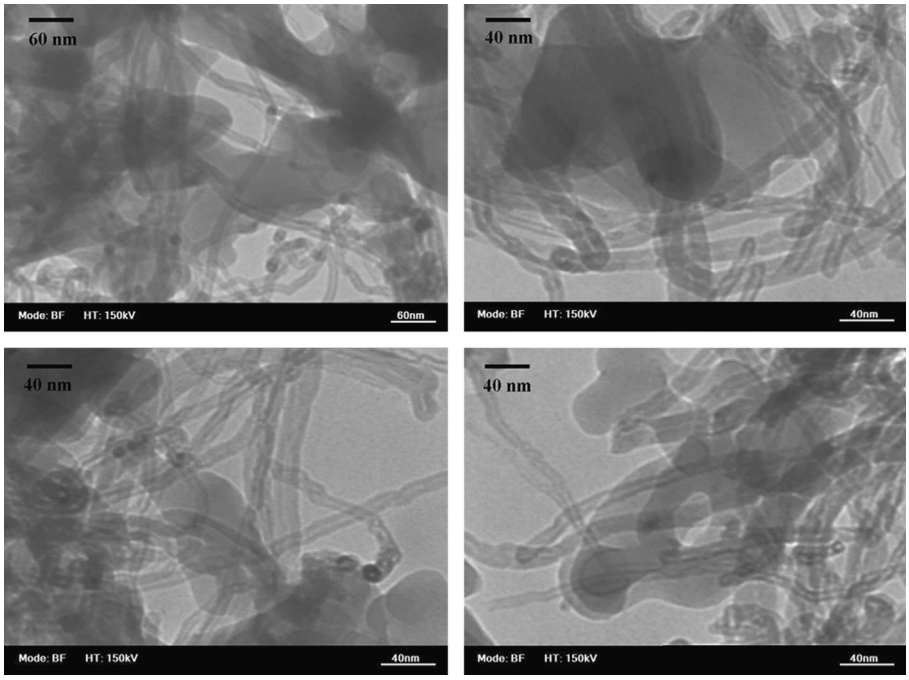

Fig. 7. TEM micrographs of MWCNTs-AS/PAI composites containing 10 wt% of MWCNT-AS.

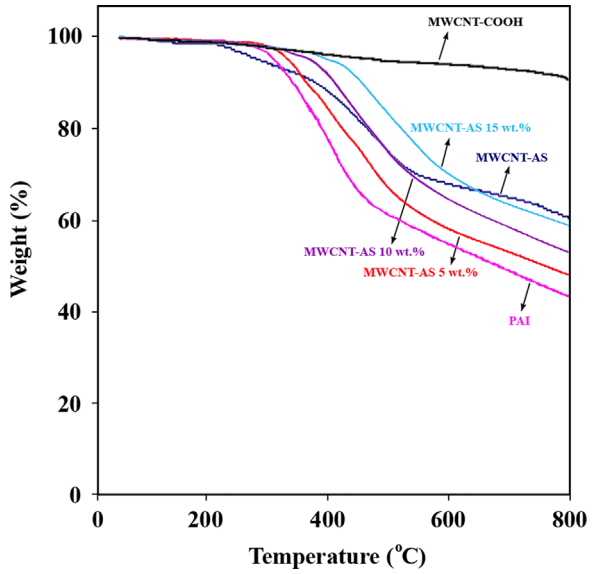

Fig. 8. TGA curves of the composites with different MWCNT-AS loading.

Table 1
Thermal stability of CNT samples obtained from TGA thermograms.[a]

Sample	T_{d5} (°C)	Weight residue at 800 °C
MWCNT-COOH	550	90
MWCNT-AS	274	60

[a] Temperature at which 5 wt% loss was recorded by TGA at a heating rate of 10 °C min^{-1} in a nitrogen atmosphere.

Therefore, it could be verified that a small amount of MWCNT acted as effective thermal degradation resistant reinforcement in the PAI matrix, increasing the thermal stability of the MWCNT/PAI composites.

The limiting oxygen index (LOI) is the minimum concentration of oxygen, expressed as a percentage, which will support combustion of a polymer. It can be used to evaluate the flame retardancy of the polymers. Normal atmospheric air is approximately 21% oxygen, so a material with an LOI of less than 21% would burn easily in air. That being said, a material with LOI of greater than 21% but less than 28% would be considered "slow burning". A material with LOI of greater than 28% would be considered "self-extinguising". A self-extinguishing material is one that would stop burning after the removal of the fire or ignition source [50].

Table 2
Thermal properties of PAI and the composites.[a]

MWCNT-AS content (%)	T_{d5}[a] (°C)	T_{d10}[a] (°C)	CR (%)[b]	LOI (%)[c]	ΔH_{comb} (kJ/g)[d]
0	315	354	43	34.7	23.0
5	340	368	47	36.3	22.0
10	374	405	52	39.1	20.4
15	403	437	58	41.5	19.3

[a] Temperature at which 5 and 10 wt% loss was recorded by TGA at a heating rate of 10 °C min^{-1} in a nitrogen atmosphere.
[b] Percentage weight of material left undecomposed after TGA analysis at maximum temperature 800 °C in a nitrogen atmosphere.
[c] Limiting oxygen index (LOI) evaluating at char yield at 800 °C.
[d] Heat of combustion, calculated from LOI.

Theoretically, two interesting relationships have been found between the LOI and the parameters of the combustion process: char yield or char residue (CR) and heat of combustion.

According to Van Krevelen [51]. There is a linear relationship between LOI and CR only for halogen-free polymers (Eq. (1)):

$$LOI = 17.5 + 0.4CR \quad (1)$$

From this equation, a higher char yield will improve flame retardance. PAI and composites, containing 5, 10, and 15 wt%, had LOI values of 34.7, 36.3, 39.1, and 41.5, respectively, as calculated from their CR. On the basis of the LOI values, such materials can be classified as self-extinguishing materials.

According to Johnson [52], the LOI values of many common materials can be logically well predicted by the expression as follows:

$$LOI = 8000/\Delta H_{comb} \quad (2)$$

where ΔH_{comb} is the specific heat of combustion in J/g. So, in the case of PAI and MWCNT/PAI composites (5, 10, and 15 wt%), ΔH_{comb} is 23.0, 22.0, 20.4, and 19.3 kJ/g, respectively.

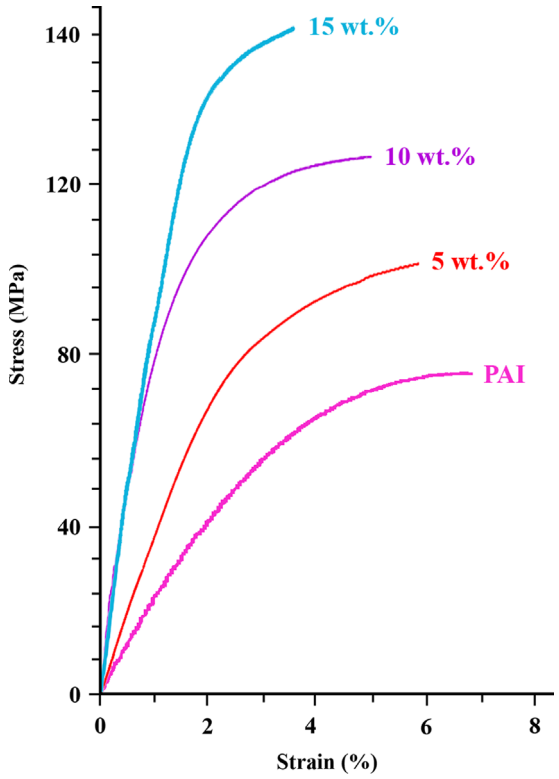

Fig. 9. Typical stress–strain curves of the composite films.

Table 3
Mechanical properties of MWCNT-AS/PAI composite films.

MWCNT-AS content (%)	Tensile strength (MPa)	Young's modulus (GPa)	Elongation at break (%)
0	75.0 ± 0.2	2.1 ± 0.1	7.3 ± 0.4
5	102.2 ± 0.2	2.9 ± 0.1	5.9 ± 0.3
10	127.5 ± 0.2	3.5 ± 0.1	5.0 ± 0.5
15	143.1 ± 0.3	4.0 ± 0.1	3.6 ± 0.3

3.5.6. *Mechanical properties*

Fig. 9 shows the tensile properties of the MWCNT/PAI composites. The tensile strength and the strain at tensile strength varied depending on the amount of MWCNTs present (Table 3). The physical interpretation for such an occurrence is that the MWCNTs were homogenously oriented in the composite, and the fraction of MWCNTs oriented in the direction of the tensile force applied was not sufficient to have an impact on Young's modulus. However, as the sample was stretched, the CNTs are gradually aligned in the direction under tensile testing and thus reinforce the material against the fracture. The more MWCNTs were added to the composite, the bigger was the reinforcement and the higher was the strain. Furthermore, the incorporation of the ascorbic acid molecules on the surface of MWCNTs and several functional groups into the PAI matrix resulted in the good interfacial adhesion between the MWCNT-AS and the PAI matrix. Therefore, the improvement of the mechanical properties of the MWCNT/PAI composites could be attributed to the better interfacial interaction between the MWCNTs-AS and the PAI matrix as well as the better dispersion of the MWCNTs-AS in the PAI matrix. The value in 102.2 MPa for the sample with 5 wt% MWCNTs-AS loading was 36.3% higher than that of the pure PAI. The elongation at the break of composite films was decreased with the introduction of MWCNT, indicating that the composites became somewhat brittle when compared with pure PAI because of the increased stiffness of the composites. This phenomenon has also been observed in other CNTs reinforced polymer systems [53,54].

4. Conclusions

In an efficient, simple and low cost strategy involving the use of microwave technology, covalent functionalization of MWCNTs with ascorbic acid was used as a means of improving the state of dispersion of MWCNTs in the polymer matrix. Functionalization was followed by reaction with a carboxylic acid moiety allows direct attachment by an ester bond. The occurrence of ascorbic acid-functionalization of the nanotubes was confirmed by the use of several methods usually used in materials science such as FT-IR, XRD, FE-SEM, TEM, and TGA. The as-prepared MWCNTs-AS were dispersed throughout a aminophenol and amino acid containing PAI. Through ultrasonically-assisted solution casting of these dispersions, MWCNT-AS/PAI composite films were successfully fabricated on substrates. The attached ascorbic acid molecules were expected to improve the interaction between the modified MWCNTs and polymer molecule chains. The composites prepared with combined functionalization or ultrasonic treatment showed substantially increased mechanical and thermal properties with increasing MWCNT content, indicative of good dispersion of MWCNTs. The results of the tensile mechanical tests showed that the tensile strength remarkably increased from 75 to 102.2 MPa, which was about 36% higher than that of neat PAI, with the addition of MWCNT-AS contents within 5 wt%. The decomposition temperatures (T_{d5} and T_{d10}) was also delayed with the increasing MWCNT-AS content in the PAI matrix. The significant improvements effects are due to the reinforcement of finely dispersed MWCNTs fillers throughout the matrix as well as the strong hydrogen interaction between carbonyl and hydroxyl groups on the surface of MWCNTs-AS and functional groups in the PAI structure, thus being favorable to stress transfer from polymer to CNTs. The obtained results from TEM showed that the MWCNTs-AS were wrapped around PAI particles and MWCNTs-AS were also mixed well with the PAI matrix, leading to the fine dispersal of MWCNTs-AS in the PAI matrix.

Acknowledgments

We are grateful to the Research Affairs Division of Isfahan University of Technology (IUT), National Elite Foundation (NEF), and Center of Excellency in Sensors and Green Chemistry Research (IUT).

References

[1] S. Iijima, Nature 354 (1991) 56–58.
[2] R.H. Baughman, A.A. Zakhidov, W.A. de Heer, Science 297 (2002) 787–792.
[3] A.C. Dillon, K. Jones, T. Bekkedahl, C. Kiang, D. Bethune, M. Heben, Nature 386 (1997) 377–379.
[4] A.D. Franklin, M. Luisier, S.-J. Han, G. Tulevski, C.M. Breslin, L. Gignac, M.S. Lundstrom, W. Haensch, Nano Lett. 12 (2012) 758–762.
[5] T. Kawano, H.C. Chiamori, M. Suter, Q. Zhou, B.D. Sosnowchik, L. Lin, Nano Lett. 7 (2007) 3686–3690.
[6] F. Valentini, L.G. Fernàndez, E. Tamburri, G. Palleschi, Biosens. Bioelectron. 43 (2013) 75–78.
[7] S. Yin, P.K. Shen, S. Song, S.P. Jiang, Electrochim. Acta 54 (2009) 6954–6958.
[8] Z. Spitalsky, D. Tasis, K. Papagelis, C. Galiotis, Prog. Polym. Sci. 35 (2010) 357–401.
[9] J. Bell, M. Giulianini, R. Goh, N. Motta, E. Waclawik, Mater. Forum (2008).
[10] M. Barski, P. Kędziora, M. Chwał, Key Eng. Mater. 542 (2013) 29–42.
[11] L-L. Ke, J. Yang, S. Kitipornchai, Mech. Adv. Mater. Struct. 20 (2013) 28–37.
[12] J. Baur, E. Silverman, MRS Bull. 32 (2007) 328–334.
[13] B. Safadi, R. Andrews, E. Grulke, J. Appl. Polym. Sci. 84 (2002) 2660–2669.
[14] X. Gui, J. Wei, K. Wang, A. Cao, H. Zhu, Y. Jia, Q. Shu, D. Wu, Adv. Mater. 22 (2010) 617–621.

[15] N. Kamanina, S. Serov, N. Shurpo, S. Likhomanova, D. Timonin, P. Kuzhakov, N. Rozhkova, I. Kityk, K. Plucinski, D. Uskokovic, J. Mater. Sci.: Mater. Electron. 23 (2012) 1538–1542.
[16] N. Kamanina, P.Y. Vasilyev, S. Serov, V. Savinov, K.Y. BogdanovD. Uskokovic, Acta Phys. Pol. A 117 (2010) 786.
[17] N. Kamanina, S. Serov, V. Savinov, Tech. Phys. Lett. 36 (2010) 40–42.
[18] T. Connolly, R.C. Smith, Y. Hernandez, Y. Gun'ko, J.N. Coleman, J.D. Carey, Small 5 (2009) 826–831.
[19] W. Bauhofer, J.Z. Kovacs, Compos. Sci. Technol. 69 (2009) 1486–1498.
[20] M.L. Gupta, S.A. Sydlik, J.M. Schnorr, D.J. Woo, S. Osswald, T.M. Swager, D. Raghavan, J. Polym. Sci. Part B: Polym. Phys. 51 (2013) 410–420.
[21] E.N. Konyushenko, J. Stejskal, M. Trchová, J. Hradil, J. Kovářová, J. Prokeš, M. Cieslar, J.-Y. Hwang, K.-H. Chen, I. Sapurina, Polymer 47 (2006) 5715–5723.
[22] F.-L. Jin, K. Yop Rhee, S.-J. Park, J. Solid State Chem. 184 (2011) 3253–3256.
[23] M. Ran, W. Sun, Y. Liu, W. Chu, C. Jiang, J. Solid State Chem. 197 (2013) 517–522.
[24] A. Zhang, M. Tang, J. Luan, J. Li, Mater. Lett. 67 (2012) 283–285.
[25] C. Baudot, C.M. Tan, Carbon 49 (2011) 2362–2369.
[26] S. Das, F. Irin, H.S. Tanvir Ahmed, A.B. Cortinas, A.S. Wajid, D. Parviz, A.F. Jankowski, M. Kato, M.J. Green, Polymer 53 (2012) 2485–2494.
[27] H. Padh, Biochem. Cell Biol. 68 (1990) 1166–1173.
[28] W.v.B. Robertson, B. Schwartz, J. Biol. Chem. 201 (1953) 689–696.
[29] G.C. Mills, J. Biol. Chem. 229 (1957) 189–197.
[30] N. Smirnoff, G.L. Wheeler, Crit. Rev. Biochem. Mol. Biol. 35 (2000) 291–314.
[31] S. Mallakpour, A.-R. Hajipour, M.H. Shahmohammadi, Iran. Polym. J. 11 (2002) 425–431.
[32] I. In, S.Y. Kim, Macromol. Chem. Phys. 206 (2005) 1862–1869.
[33] S. Mallakpour, A. Zadehnazari, Adv. Polym. Technol. 32 (2013) 21333.
[34] S. Mallakpour, A. Zadehnazari, Synth. Met. 169 (2013) 1–11.
[35] S. Mallakpour, A. Zadehnazari, J. Polym. Res. 20 (2013) 1–12.
[36] S. Mallakpour, A. Zadehnazari, High. Perform. Polym. 25 (2013) 966–979.
[37] S. Mallakpour, A. Zadehnazari, Polymer 54 (2013) 6329–6338.
[38] S. Mallakpour, A. Zadehnazari, Polym. Int. (2013), http://dx.doi.org/10.1002/pi.4622, in press.
[39] J.F. Vega, J. Martínez-Salazar, M. Trujillo, M.L. Arnal, A.J. Müller, S. Bredeau, P. Dubois, Macromolecules 42 (2009) 4719–4727.
[40] S. Mallakpour, A. Zadehnazari, Carbon 56 (2013) 27–37.
[41] Q.-P. Feng, J.-P. Yang, S.-Y. Fu, Y.-W. Mai, Carbon 48 (2010) 2057–2062.
[42] M. Mohiuddin, S. Hoa, Compos. Sci. Technol. 72 (2011) 21–27.
[43] K. Bui, B.P. Grady, D.V. Papavassiliou, Chem. Phys. Lett. 508 (2011) 248–251.
[44] H.-J. Lee, S.-J. Oh, J.-Y. Choi, J.W. Kim, J. Han, L.-S. Tan, J.-B. Baek, Chem. Mater. 17 (2005) 5057–5064.
[45] S.-H. Hsiao, W. Guo, W.-F. Lee, Y.-C. Kung, Y.-J. Lee, Mater. Chem. Phys. 130 (2011) 1086–1093.
[46] M. Perez-Cabero, I. Rodrıguez-Ramos, A. Guerrero-Ruız, J. Catal. 215 (2003) 305–316.
[47] A. Amiri, M. Maghrebi, M. Baniadam, S. Zeinali Heris, Appl. Surf. Sci. 257 (2011) 10261–10266.
[48] E. Vázquez, M. Prato, ACS Nano 3 (2009) 3819–3824.
[49] S.T. Huxtable, D.G. Cahill, S. Shenogin, L. Xue, R. Ozisik, P. Barone, M. Usrey, M.S. Strano, G. Siddons, M. Shim, Nat. Mater. 2 (2003) 731–734.
[50] P. Carty, S. White, Polymer 35 (1994) 5595–5596.
[51] D. Van Krevelen, Polymer 16 (1975) 615–620.
[52] P. Johnson, J. Appl. Polym. Sci. 18 (1974) 491–504.
[53] J.J. Ge, D. Zhang, Q. Li, H. Hou, M.J. Graham, L. Dai, F.W. Harris, S.Z. Cheng, J. Am. Chem. Soc. 127 (2005) 9984–9985.
[54] E.J. Siochi, D.C. Working, C. Park, P.T. Lillehei, J.H. Rouse, C.C. Topping, A.R. Bhattacharyya, S. Kumar, Composites Part B 35 (2004) 439–446.